Simultaneous Inversion of Unique ϕ/K Features from Production Data

Z. A. Reza (zreza@ualberta.ca) and C. V. Deutsch (cdeutsch@civil.ualberta.ca)
Department of Civil & Environmental Engineering, University of Alberta

X. H. Wen (xwen@chevrontexaco.com)
ChevronTexaco Exploration and Production Technology Company

Abstract

The ability and the effectiveness of an algorithm for simultaneous inversion of ϕ and K is addressed. We experiment with reservoir models with unique ϕ/K features, and analyze the inversion outcomes. The inverted models capture the heterogeneity in the reference models reasonably well. The effectiveness of the developed algorithm compared to others available in the literature are discussed.

Simultaneous Inversion of Unique $\phi/\ln(k)$ Features From Production Data

We presented an algorithm for simultaneous inversion of ϕ and K in [1]. The ability and the effectiveness of the algorithm was discussed in [1]. In this paper, we analyze the inversion experiment with reservoir models with unique $\phi/\ln(k)$ features.

A Synthetic Reservoir Model with Unique $\phi/\ln(k)$ Features

Consider a 2D example of 4,000 ft by 4,000 ft domain that is discretized into 40 $\times$ 40 grid cells of 100 $\times$ 100 ft. Porosity and permeability fields are shown in Figure 1. It is evident from the figure that reference porosity field has large continuity in the North-South direction. Porosity values gradually decrease in the Westward direction. Whereas, the permeability field has large continuity in Southwest-Northeast direction. In the Southeast portion of the reservoir the permeability values are high. Permeability decreases gradually in Northeastward direction. There are 8 wells: W1 at the center of the cell (34,33), W2 at (33,8), W3 at (25,12), W4 (18,27), W5 (14,6), W6 (30,17), W7 (8,33), and W8 (35,12), respectively. Wells are shown in Figure 1. The four boundaries are no-flow boundaries, reservoir thickness is 100 ft, viscosity is 0.2 cp, formation compressibility is 10^{-6} psi^{-1}, and well radius is 0.3 ft. Figure 2 shows the imposed production rates and the corresponding numerically simulated pressure responses at the different wells. The global histograms of the reference distributions and the scatter-plot between porosity and $\ln(k)$ are shown in Figures 3 and 4, respectively. Mean and standard deviation of reference distributions are 0.129 and 0.056 for ϕ, and 1.33 and 1.608 for $\ln(k)$. The low average porosity confirms the low storativity of the reservoir. Correlation coefficient of the two distributions is 0.31. Variogram for both ϕ and $\ln(k)$ of the reference fields are shown in Figure 5.

We employ the reference distributions as the global distribution information. It is true that we do not have this information a priori, in that case we could use an approximate global distribution informed by some secondary data such as seismic data. Static well data used in the example are shown in Figure 6. We perform the inversion with a number of prior variogram models and analyze the inverted models in each of the runs.

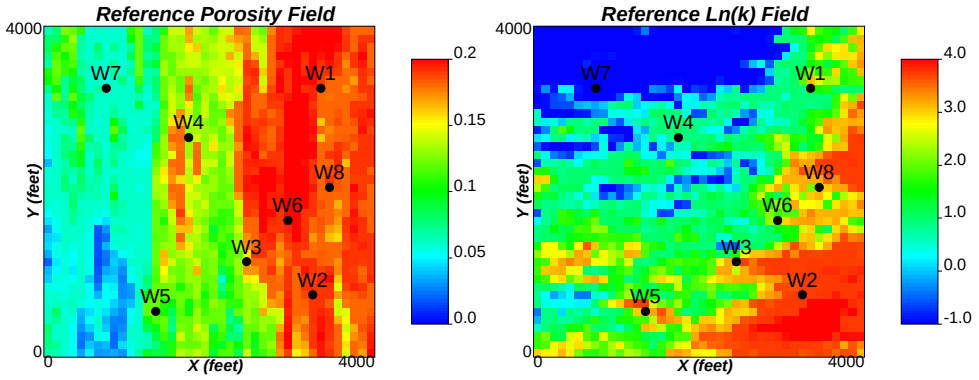

Figure 1: Reference ϕ and $\ln(k)$ fields.

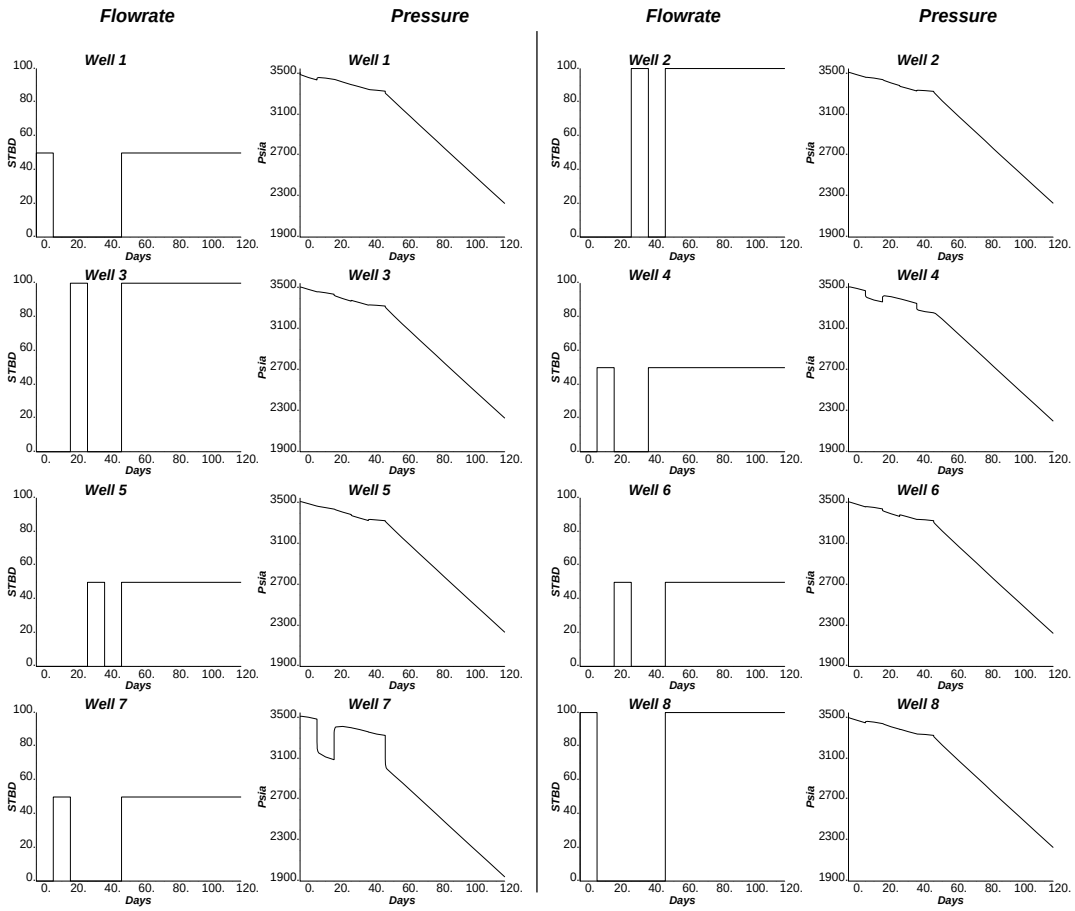

Figure 2: Production data (pressure and flow rates) obtained for 8 wells from the reference field.

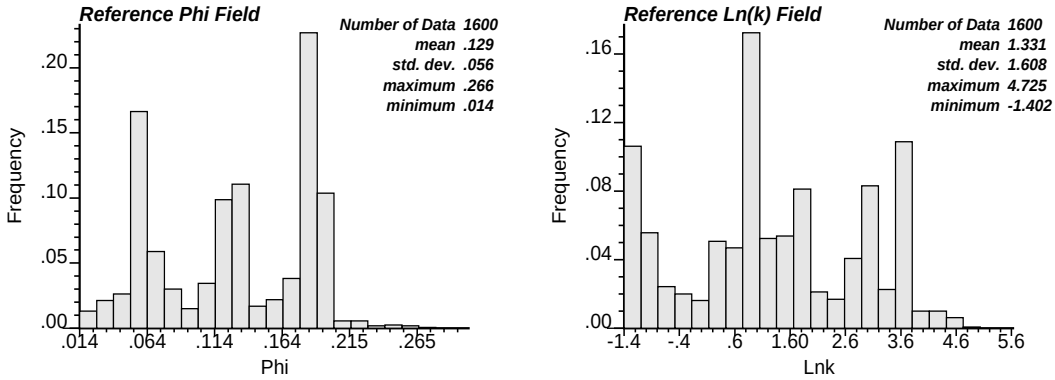

Figure 3: Histograms of reference ϕ and $\ln(k)$ fields.

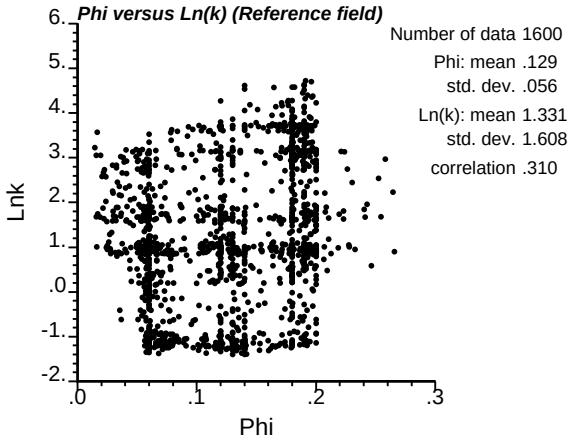

Figure 4: Scatterplot of reference ϕ and $\ln(k)$ values.

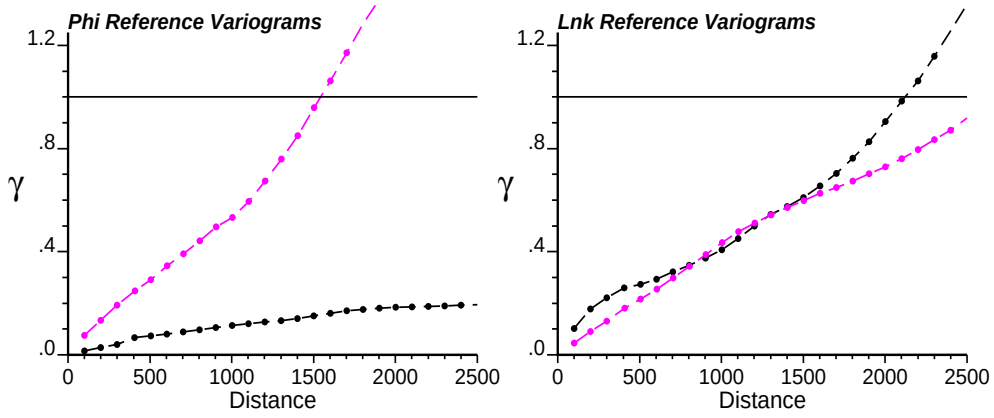

Figure 5: Variograms of reference ϕ and $\ln(k)$. (X direction - light, Y direction - dark)

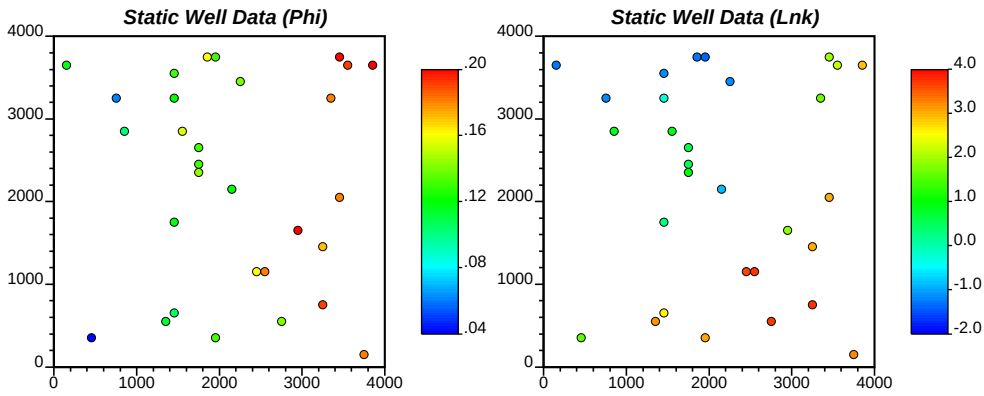

Figure 6: Static well data for ϕ and $\ln(k)$.

V. No.	**Type**	**Sill**	**Range** X - Y (ft)	**Angle** (^{o})
0	Nugget	0.05		
1	Sph	0.55	14000 - 4000	0
2	Sph	0.4	13000 - 10000	0

Table 1: Prior variogram information used for ϕ: Run 1.

Run 1

The prior variogram model used in this run is shown in Tables 1 and 2 for ϕ and $\ln(k)$. The inversion was run for 16 outer iterations using 6×6 (=36) master points in each iteration. CPU time for the run was only 315 seconds in a 1.8 GHz Pentium 4 machine. The pressure responses in the updated porosity and permeability fields converge to the reference pressure data. These inverted models are shown in Figure 7. Figure 8 shows the pressure values at the eight wells computed from the true (from reference), initial and final updated porosity and permeability fields. The updated fields by the new method accurately reproduce the true pressure data at all wells except Well W4 which is located at (1750.0, 2650.0). The objective function values of the inversion process are shown in Figure 9. Final average pressure mismatch in L^2 norm sense was 14.7 psi. Updated porosity and permeability fields after each outer iteration of the inversion method are shown in Figures 10 and 11.

Run 2

The prior variogram model used in this run is shown in Tables 3 and 4 for ϕ and $\ln(k)$. The inversion was run for 17 outer iterations using 6×6 (=36) master points in each iteration. CPU time for the run was only 331 seconds in a 1.8 GHz Pentium 4 machine. The pressure responses in the updated porosity and permeability fields converge to the reference pressure data. These inverted models are shown in Figure 12. Figure 13 shows the pressure values at the eight wells computed from the true (from reference), initial and final updated porosity and permeability fields. The updated fields by the new method accurately reproduce the true pressure data at all wells except the same Well W4

V. No.	**Type**	**Sill**	**Range** X - Y (ft)	**Angle** (^{o})
0	Nugget	0.05		
1	Sph	0.5	14000 - 9000	0
2	Sph	0.45	13000 - 10000	0

Table 2: Prior variogram information used for both $\ln(k)$: Run 1.

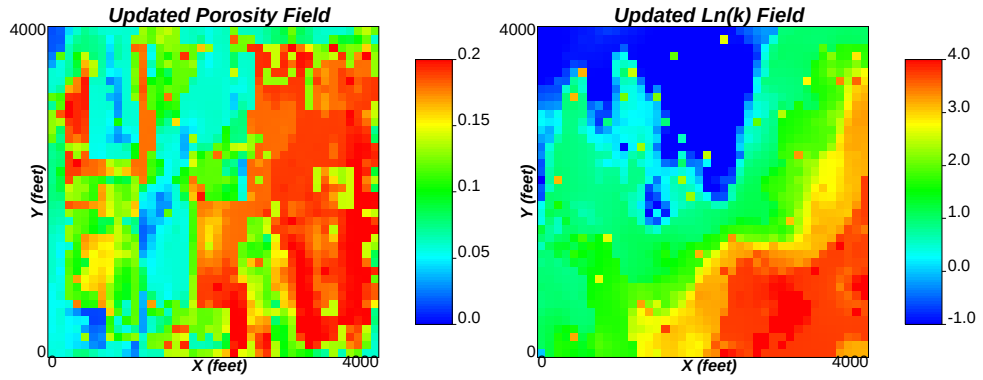

Figure 7: Updated ϕ and $\ln(k)$ fields: Run 1.

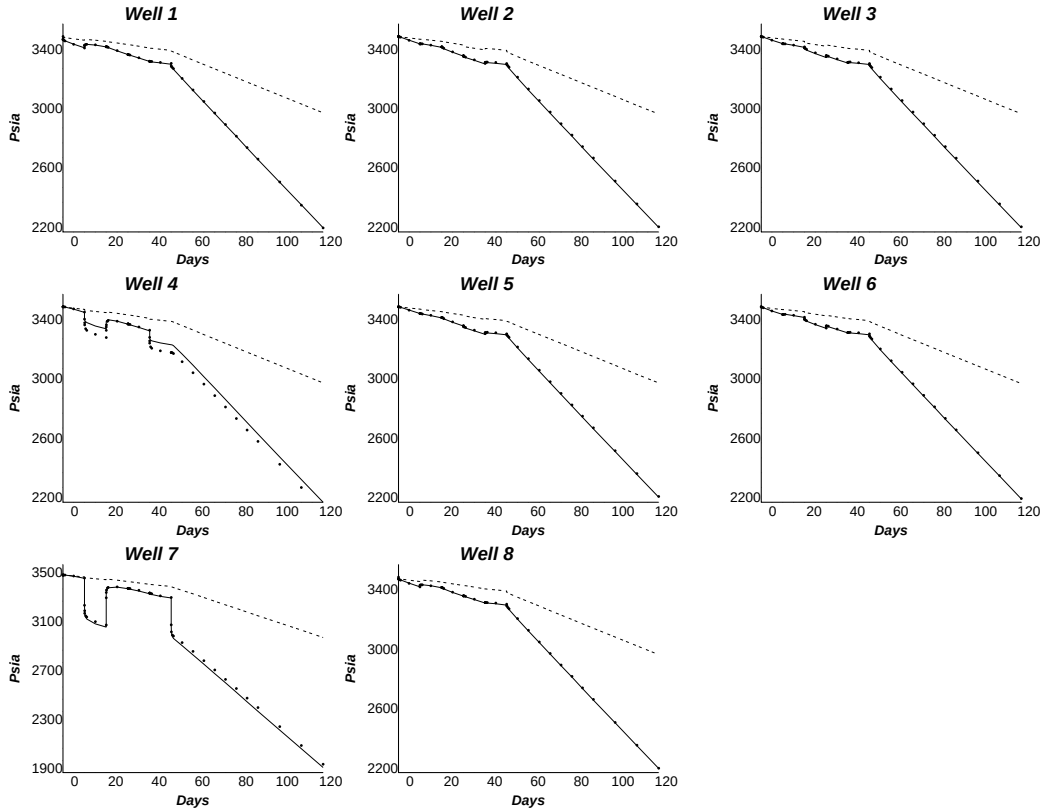

Figure 8: Pressure responses computed from initial (dashed lines) and updated (bullets) ϕ and $\ln(k)$ fields with the true data (solid lines): Run 1.

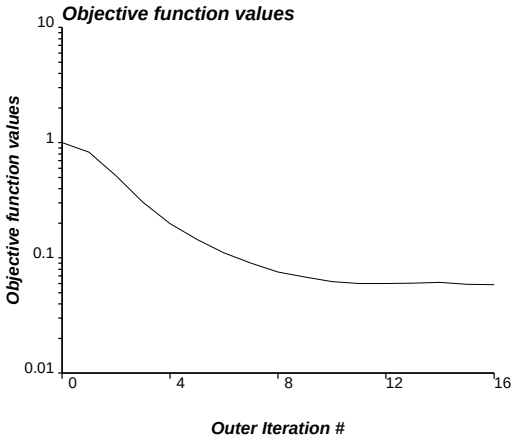

Figure 9: Objective function values of the inversion process: Run 1.

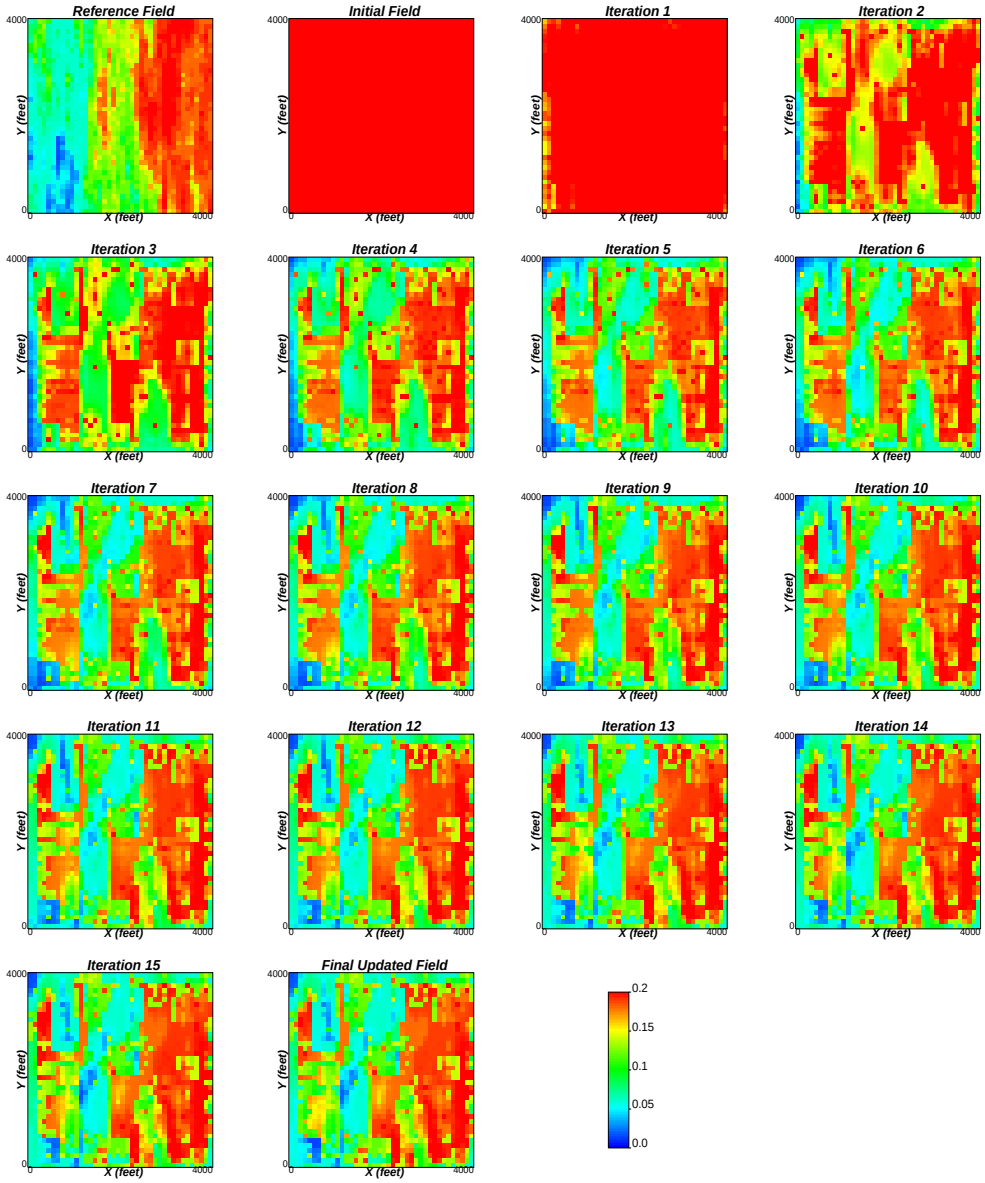

Figure 10: Updated ϕ fields at each iteration of the inversion process: Run 1.

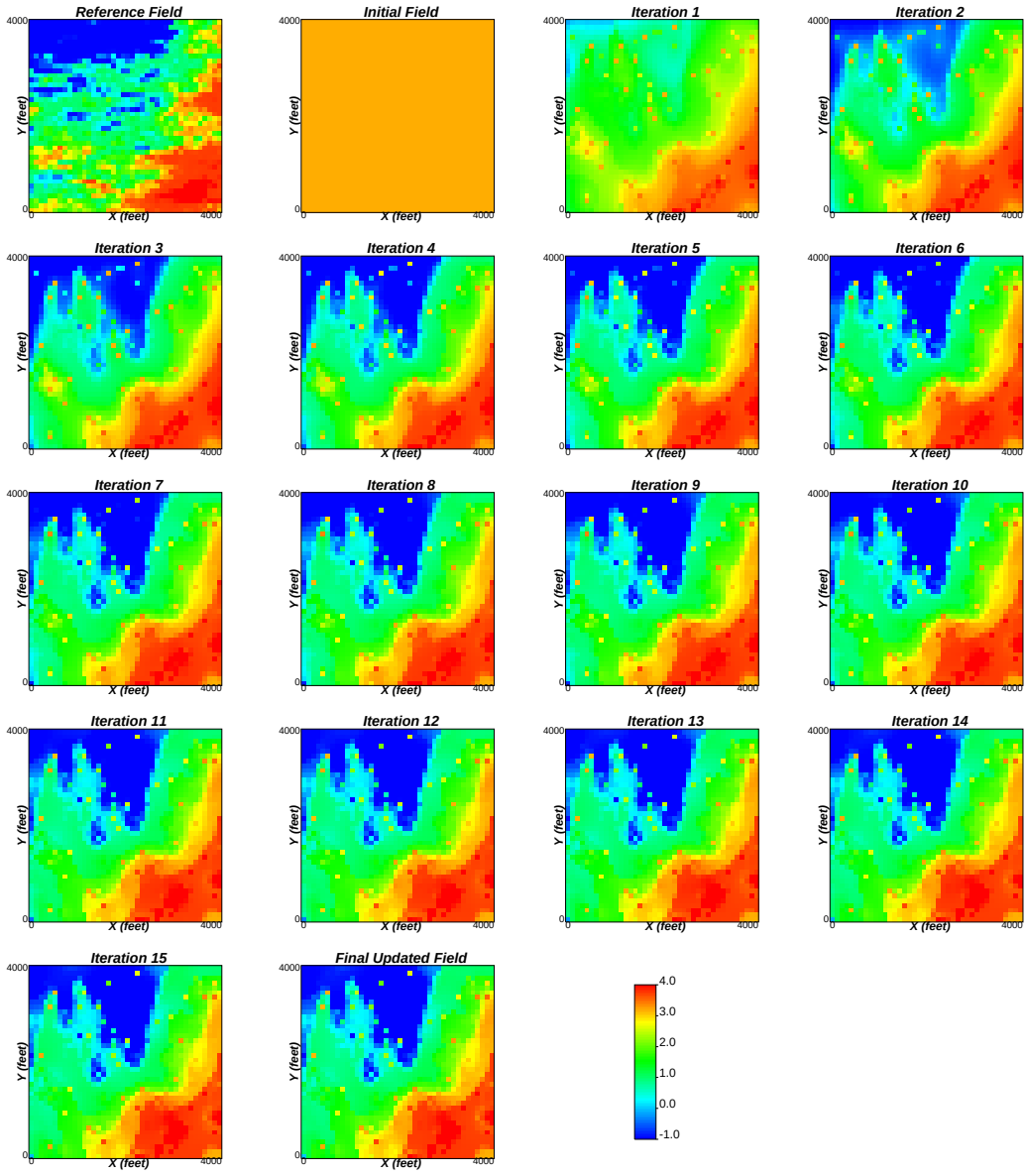

Figure 11: Updated $\ln(k)$ fields at each iteration of the inversion process: Run 1.

V. No.	Type	Sill	Range X - Y (ft)	Angle (^{o})
0	Nugget	0.05		
1	Sph	0.55	4000 - 10000	0
2	Sph	0.4	10000 - 12000	0

Table 3: Prior variogram information used for ϕ: Run 2.

V. No.	Type	Sill	Range X - Y (ft)	Angle (^{o})
0	Nugget	0.05		
1	Sph	0.5	4000 - 9000	0
2	Sph	0.45	10000 - 10000	0

Table 4: Prior variogram information used for $\ln(k)$: Run 2.

as in Run 1. However, the mismatch in this case has reduced. The objective function values of the inversion process are shown in Figure 14. Final average pressure mismatch in L^2 norm sense was 12.5 psi. Updated porosity and permeability fields after each outer iteration of the inversion method are shown in Figures 15 and 16.

Having analyzed the inverted models from the two runs, it could be concluded that the algorithm provides reasonably good models. However, better models are obtained for permeability than those for porosity. In the first run, we started with a prior variogram model with high continuity in the North-South direction for both ϕ and $\ln(k)$, the inverted models had right heterogeneity structure for $\ln(k)$. In the second run, we started with an almost isotropic model. In this case also we retrieve the right structure for $\ln(k)$. However, for ϕ the nugget effect is exaggerated. Well W4 (1750.0, 2650.0) in both runs had the highest mismatch. In the reference models, ϕ and $\ln(k)$ values in this grid block are 0.131 and 0.542; average values for both variables. Inspecting the inverted fields, we could see poor inverted values around this block.

Note that the termination criteria for the outer loop of the inversion algorithm are maximum number of outer iterations or a tolerance value for the objective function. If the second criterion is not met, we first perform the inversion with a large value for the number of outer iterations. Then we examine the objective function curve and in the next run we set the number of outer iterations to this value. This could be automated in the code by storing the best model and the number of outer loops, and reporting the outputs up to this outer iteration.

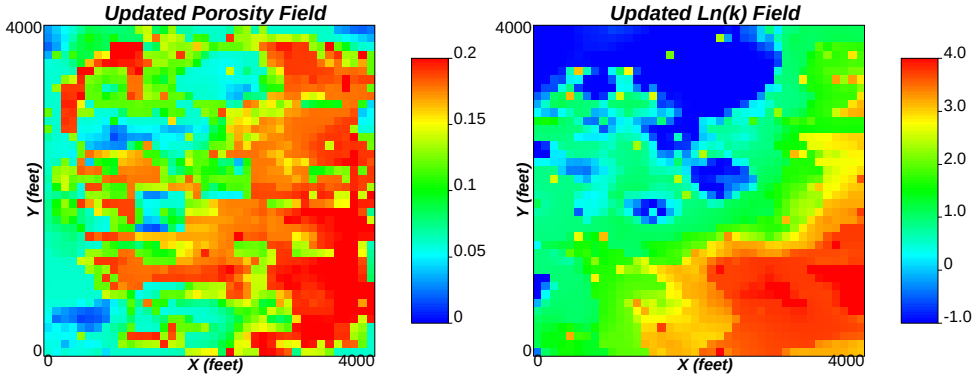

Figure 12: Updated ϕ and $\ln(k)$ fields: Run 2.

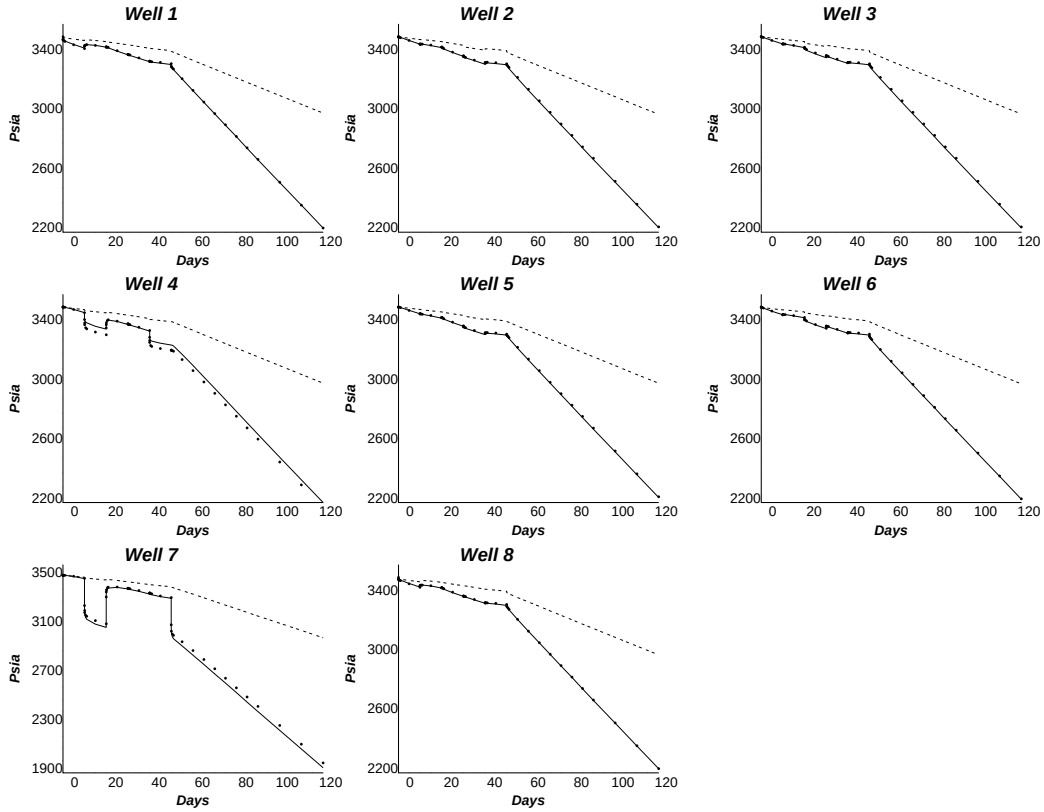

Figure 13: Pressure responses computed from initial (dashed lines) and updated (bullets) ϕ and $\ln(k)$ fields with the true data (solid lines): Run 2.

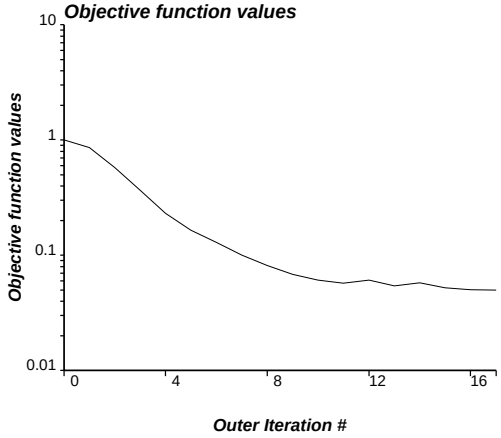

Figure 14: Objective function values of the inversion process: Run 2.

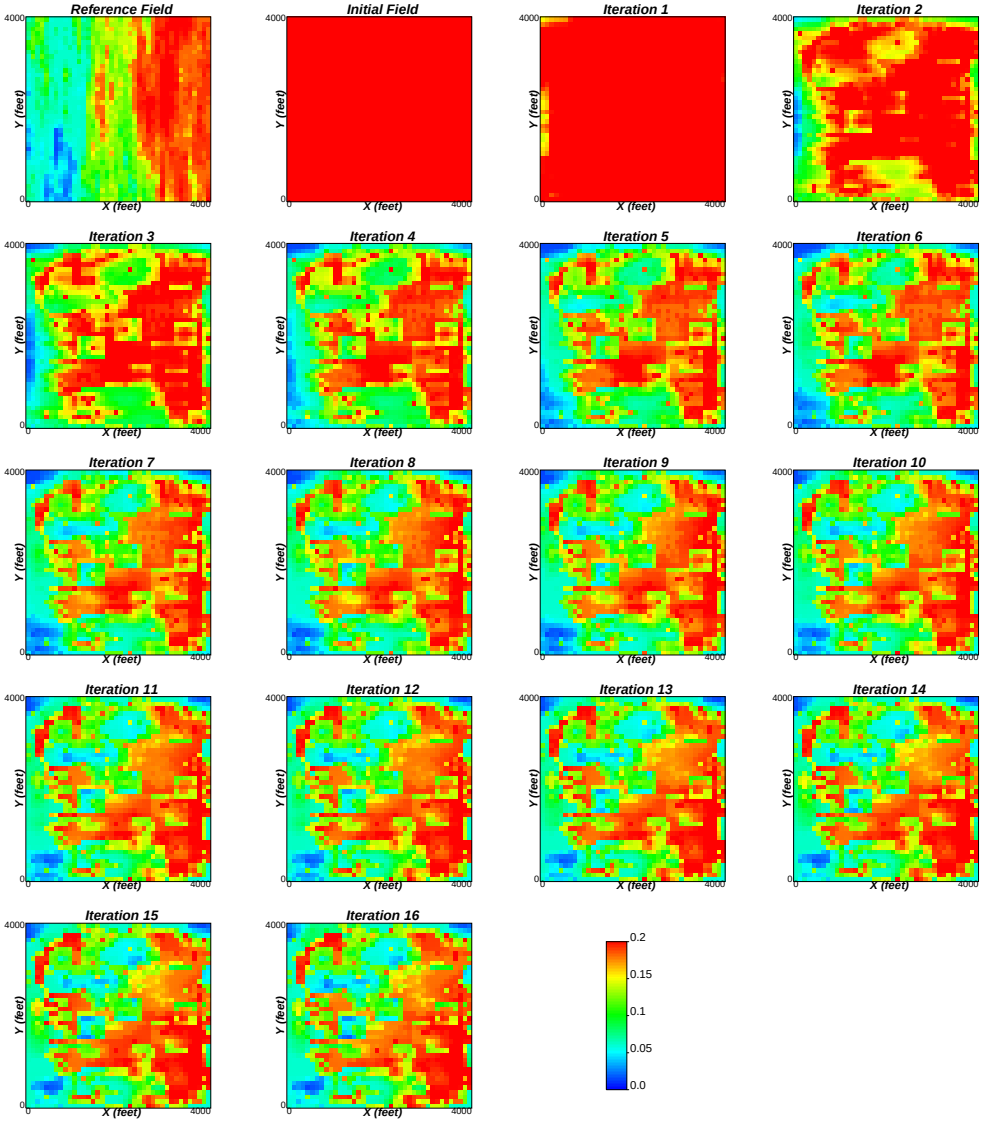

Figure 15: Updated ϕ fields at each iteration of the inversion process: Run 2.

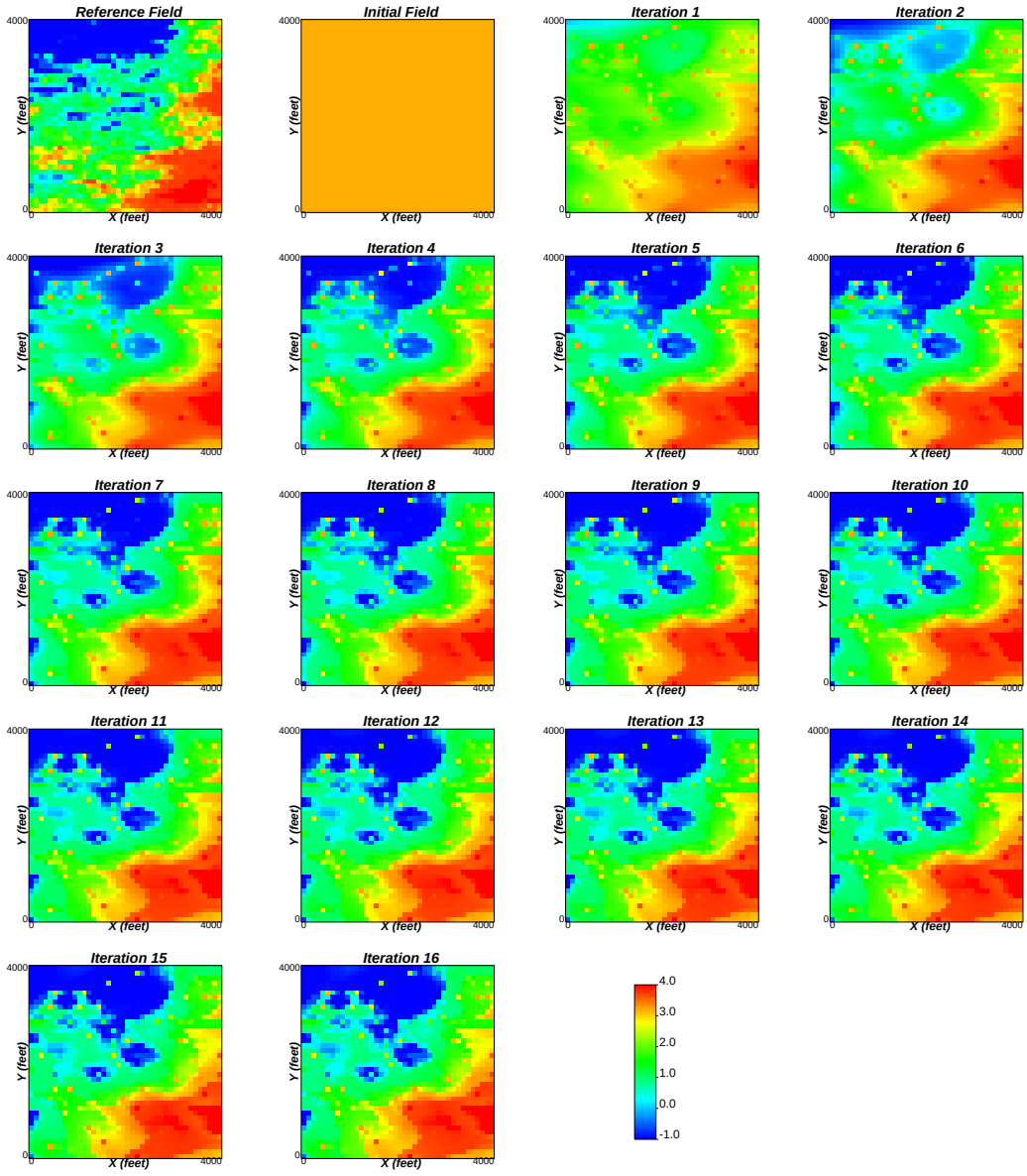

Figure 16: Updated $\ln(k)$ fields at each iteration of the inversion process: Run 2.

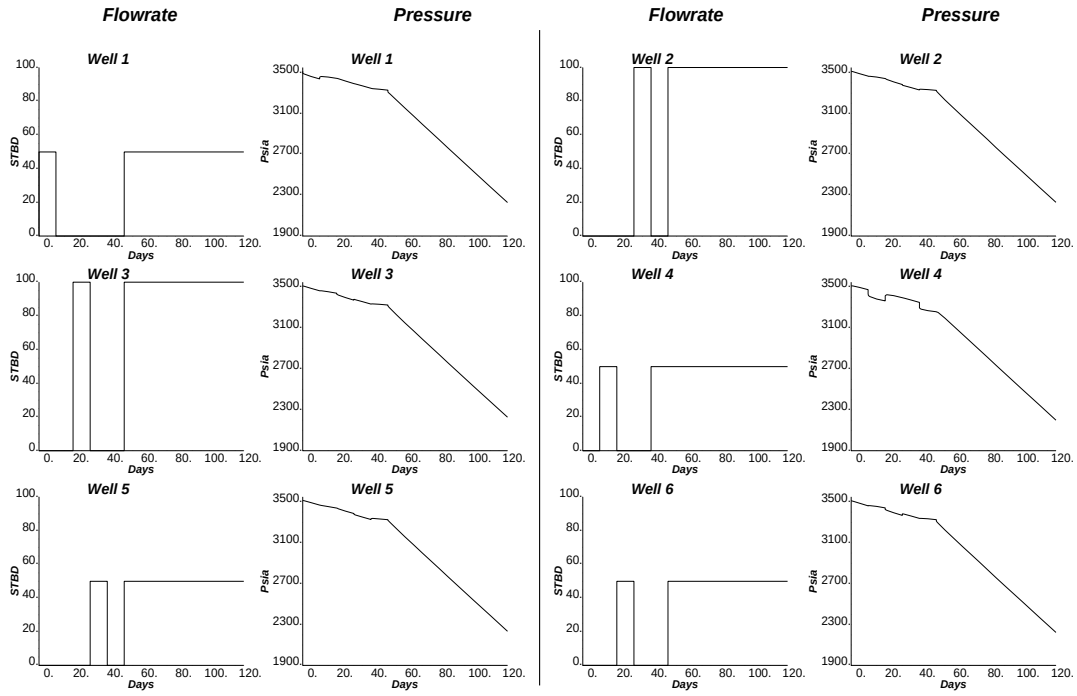

Figure 17: Production data (pressure and flow rates) obtained from the reference field: 6 Well Case.

Effect of Production Data

In this section, we investigate the effect of production data on the inversion outcome. We reduce the number of wells to 6 and 4, and perform the inversion. We employ similar parameters as in the previous section apart from the production data.

6 Well Case

The 6 wells are: W1 at the center of the cell (34,33), W2 at (33,8), W3 at (25,12), W4 (18,27), W5 (14,6), and W6 (30,17), respectively. The wells are shown in Figure 1. Figure 17 shows the imposed production rates and the corresponding numerically simulated pressure responses at these wells. The anisotropic low nugget prior variogram model used in this run is shown in Tables 3 and 4 for ϕ and $\ln(k)$. The inversion was run for 7 outer iterations using 6×6 (=36) master points in each iteration. CPU time for the run was only 143 seconds in a 1.8 GHz Pentium 4 machine. The pressure responses in the updated porosity and permeability fields converge to the reference pressure data. These inverted models are shown in Figure 18. Figure 19 shows the pressure values at the six wells computed from the true (from reference), initial and final updated porosity and permeability fields. The updated fields by the new method accurately reproduce the true pressure data at all wells except Well W4 that is located at (1750.0, 2650.0). The objective function values of the inversion process is shown in Figure 20. Final average pressure mismatch in L^2 norm sense was 6.35 psi. Updated porosity and permeability fields after each outer iteration of the inversion method are shown in Figures 21 and 22.

4 Well Case

The 4 wells are: W1 at the center of the cell (34,33), W2 at (33,8), W3 at (25,12), and W4 (18,27). The wells are shown in Figure 1. Figure 23 shows the imposed production rates and the corresponding numerically simulated pressure responses at these wells. The prior variogram model used in this run is shown in Tables 3 and 4 for ϕ and $\ln(k)$. The inversion was run for 7 outer iterations using $6 \times$

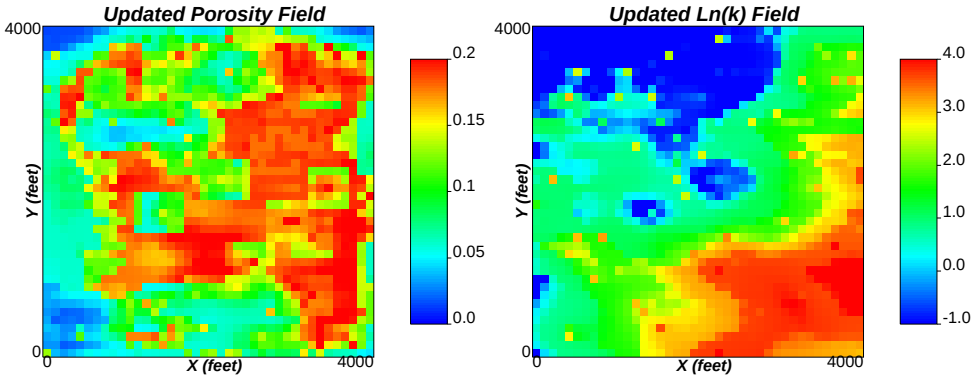

Figure 18: Updated ϕ and $\ln(k)$ fields: 6 Well Case.

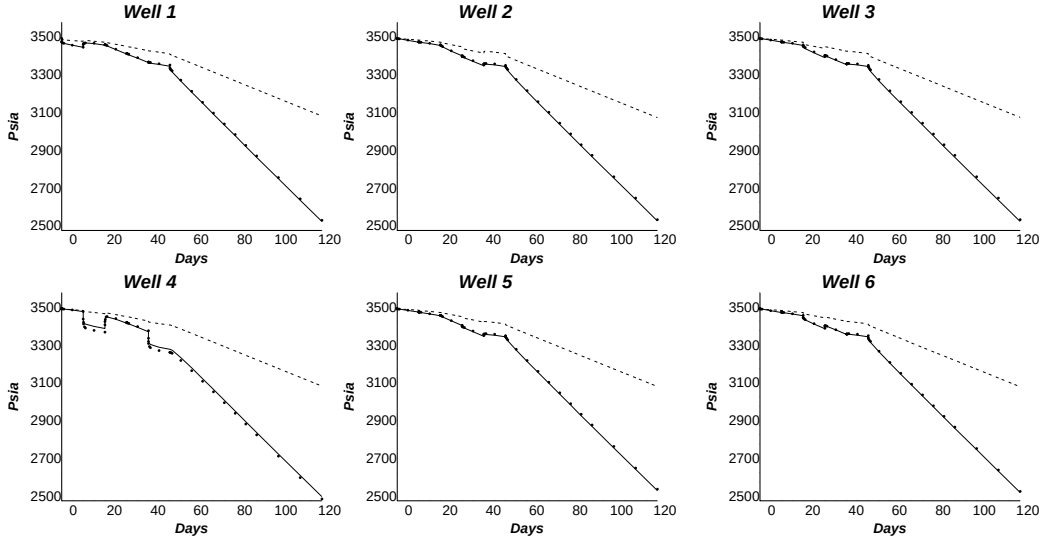

Figure 19: Pressure responses computed from initial (dashed lines) and updated (bullets) ϕ and $\ln(k)$ fields with the true data (solid lines): 6 Well Case.

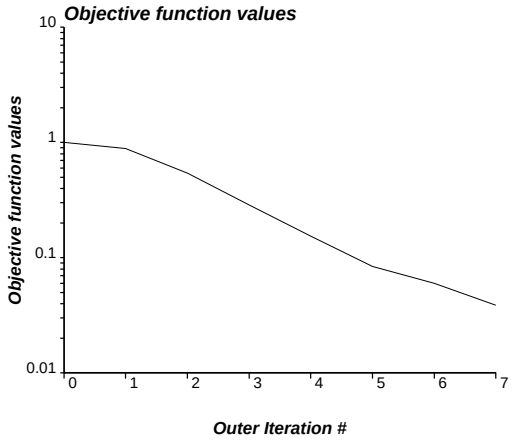

Figure 20: Objective function values of the inversion process: 6 Well Case.

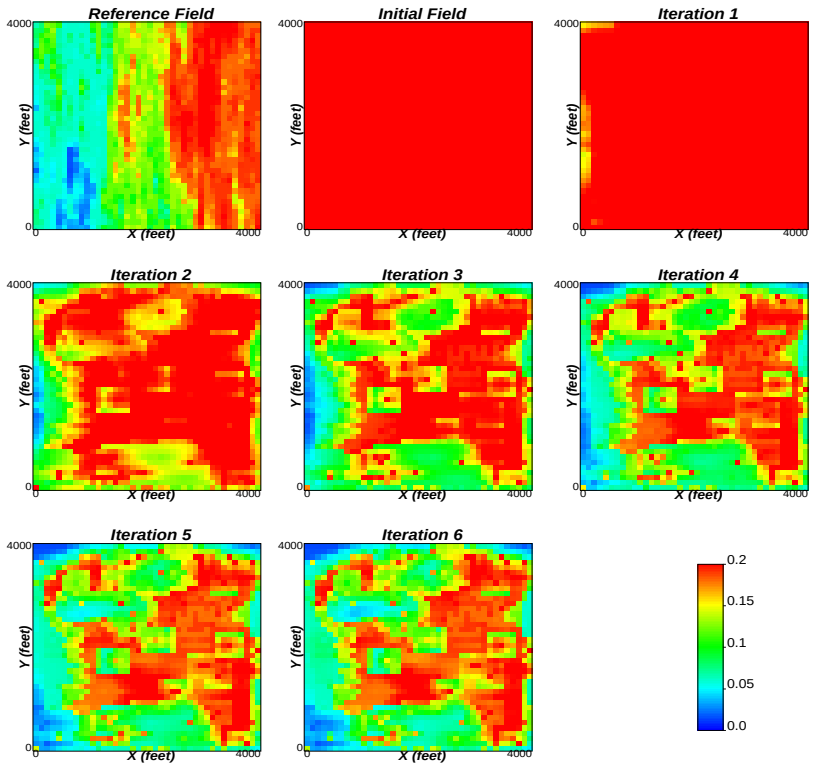

Figure 21: Updated ϕ fields at each iteration of the inversion process: 6 Well Case.

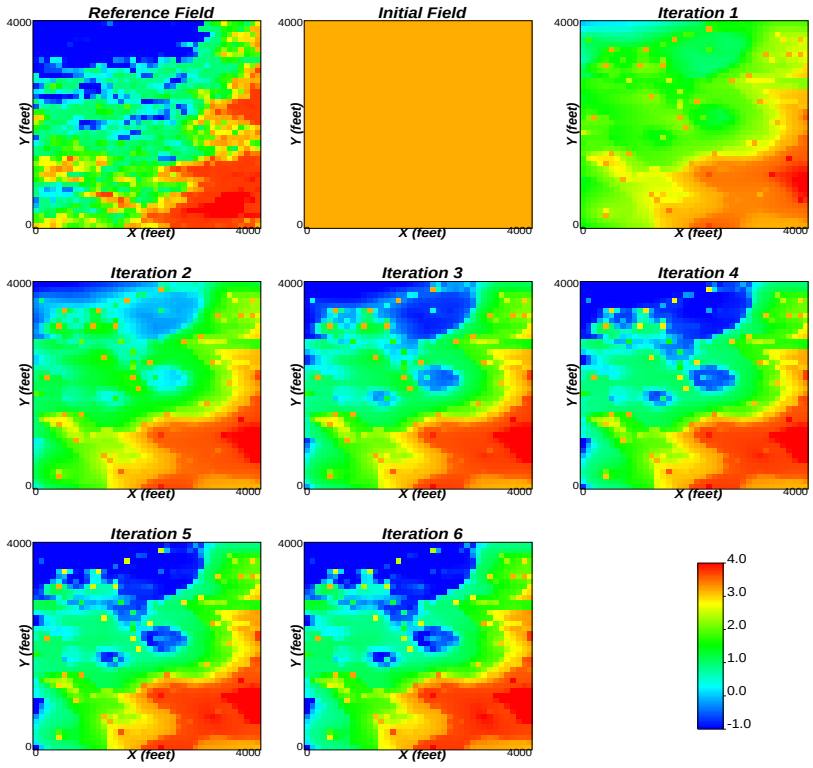

Figure 22: Updated $\ln(k)$ fields at each iteration of the inversion process: 6 Well Case.

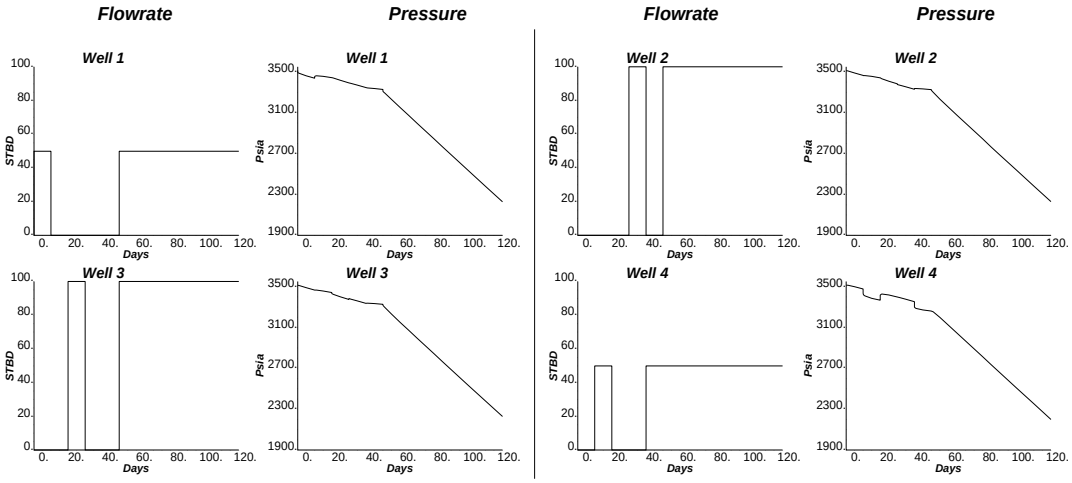

Figure 23: Production data (pressure and flow rates) obtained from the reference field: 4 Well Case.

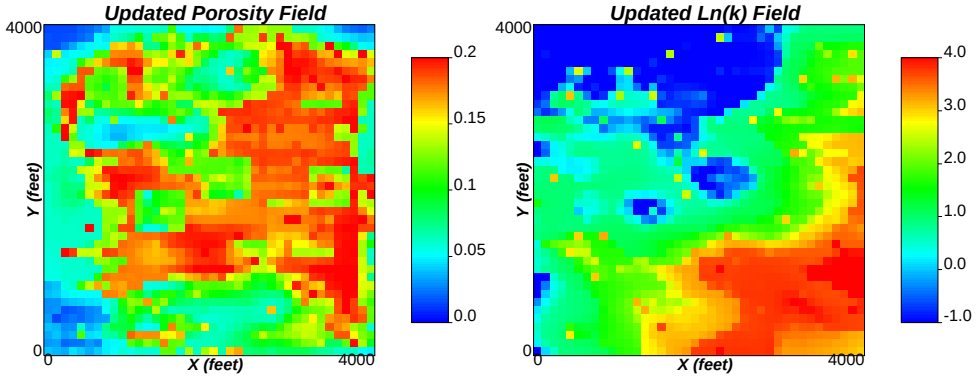

Figure 24: Updated ϕ and $\ln(k)$ fields: 4 Well Case.

6 (=36) master points in each iteration. CPU time for the run was only 143 seconds in a 1.8 GHz Pentium 4 machine. The pressure responses in the updated porosity and permeability fields converge to the reference pressure data. These inverted models are shown in Figure 24. Figure 25 shows the pressure values at the four wells computed from the true (from reference), initial and final updated porosity and permeability fields. The updated fields by the new method accurately reproduce the true pressure data at all wells except Well W4 that is located at (1750.0, 2650.0). The objective function values of the inversion process is shown in Figure 26. Final average pressure mismatch in L^2 norm sense was 7.69 psi. Updated porosity and permeability fields after each outer iteration of the inversion method are shown in Figures 27 and 28.

Conclusion

It could be concluded that using 4, 6 or 8 wells for porosity, permeability inversion leads to similar models for the present synthetic reservoir model with unique heterogeneity features. Originally, the intention was to investigate whether the developed algorithm can invert ϕ, $\ln(k)$ models where in some portions of the reservoir the correlation between the two petrophysical variables is poor. The responses of the inversion runs and the sensitivities performed confirm that it is possible to invert for this kind of models. However, it appears $\ln(k)$ models obtained through this algorithm retrieves heterogeneity features better than that of ϕ. A possible solution of this limitation may be

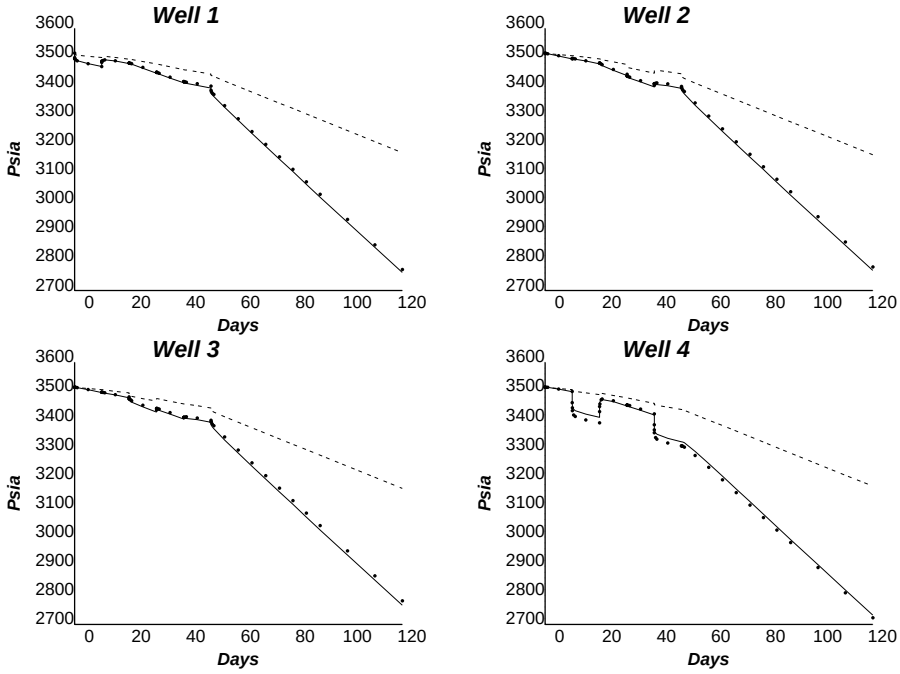

Figure 25: Pressure responses computed from initial (dashed lines) and updated (bullets) ϕ and $\ln(k)$ fields with the true data (solid lines): 4 Well Case.

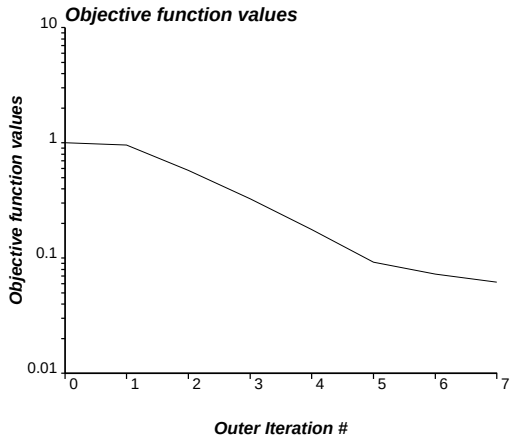

Figure 26: Objective function values of the inversion process: 4 Well Case.

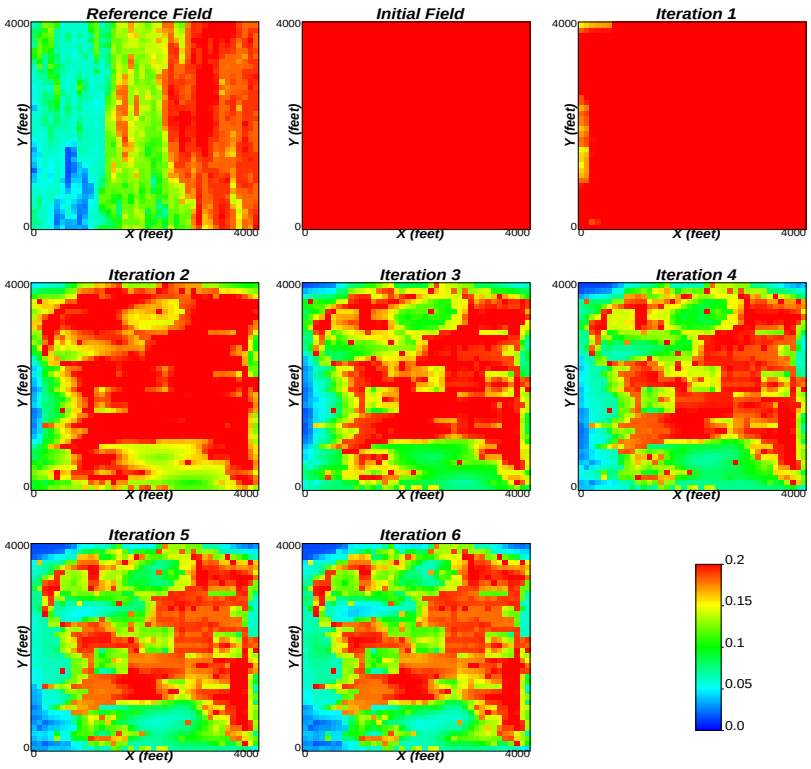

Figure 27: Updated ϕ fields at each iteration of the inversion process: 4 Well Case.

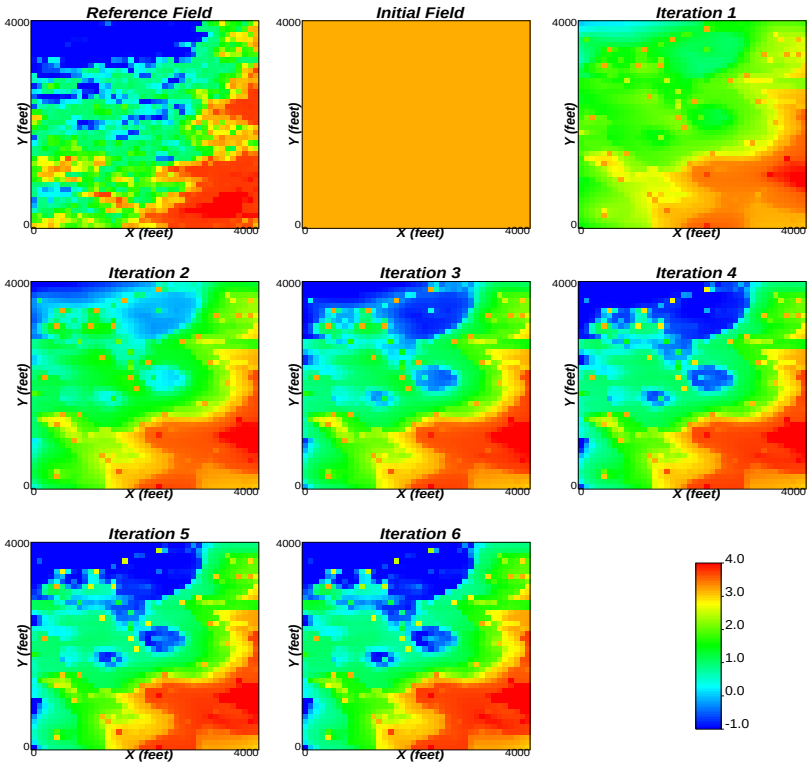

Figure 28: Updated $\ln(k)$ fields at each iteration of the inversion process: 4 Well Case.

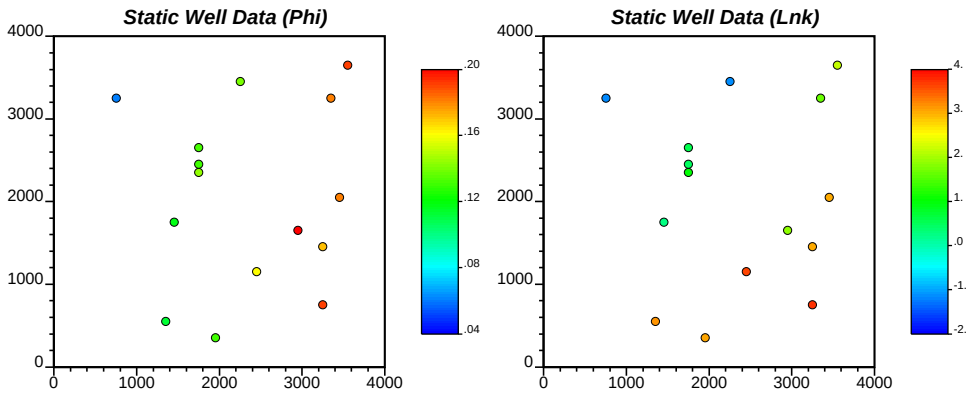

Figure 29: Static well data for ϕ and $\ln(k)$: 15 Local Data Case.

to calculate the ϕ gradients independently from the flow and constitutive equations involved.

Influence of Local Data

In all the previous inversion runs, we performed the inversion using "many" local data (30 precisely). It would be interesting to see how much incremental contribution of these local data is in the inverted models. In order to investigate this we perform the inversion by varying the number of local data to 15 and 0. We use similar parameters as used in the previous section for 6 well case. The 6 wells are: W1 at the center of the cell (34,33), W2 at (33,8), W3 at (25,12), W4 (18,27), W5 (14,6), and W6 (30,17). Wells are shown in Figure 1. Figure 17 shows the imposed production rates and the corresponding numerically simulated pressure responses at these wells. The prior variogram model used in this run is shown in Tables 3 and 4 for ϕ and $\ln(k)$.

15 Local Data Case

Local data used in this run are shown in Figure 29. The inversion was run for 6 outer iterations using 6×6 (=36) master points in each iteration. CPU time for the run was only 125 seconds in a 1.8 GHz Pentium 4 machine. The pressure responses in the updated porosity and permeability fields converge to the reference pressure data. These inverted models are shown in Figure 30. Figure 31 shows the pressure values at the six wells computed from the true (from reference), initial and final updated porosity and permeability fields. The updated fields by the new method accurately reproduce the true pressure data at all wells. Even Well W4 located at (1750.0, 2650.0) pressure match is good in this case. The objective function values of the inversion process is shown in Figure 32. Final average pressure mismatch in L^2 norm sense was 4.05 psi. This mismatch value compared to that (6.35) with 30 local data is even better. Updated porosity and permeability fields after each outer iteration of the inversion method are shown in Figures 33 and 34.

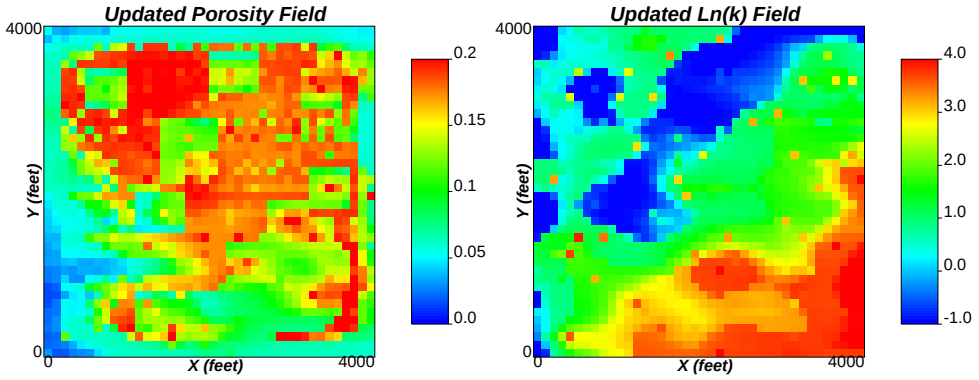

Figure 30: Updated ϕ and $\ln(k)$ fields: 15 Local Data Case.

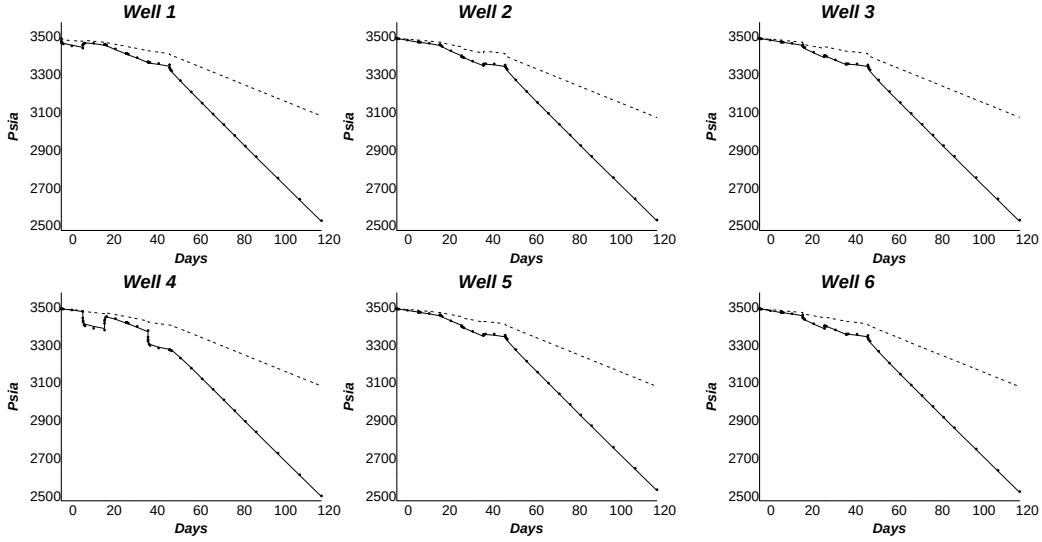

Figure 31: Pressure responses computed from initial (dashed lines) and updated (bullets) ϕ and $\ln(k)$ fields with the true data (solid lines): 15 Local Data Case.

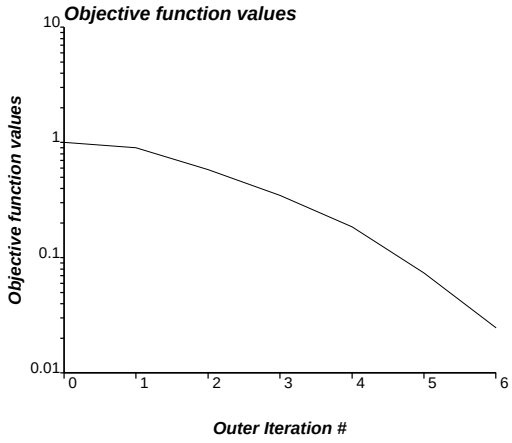

Figure 32: Objective function values of the inversion process: 15 Local Data Case.

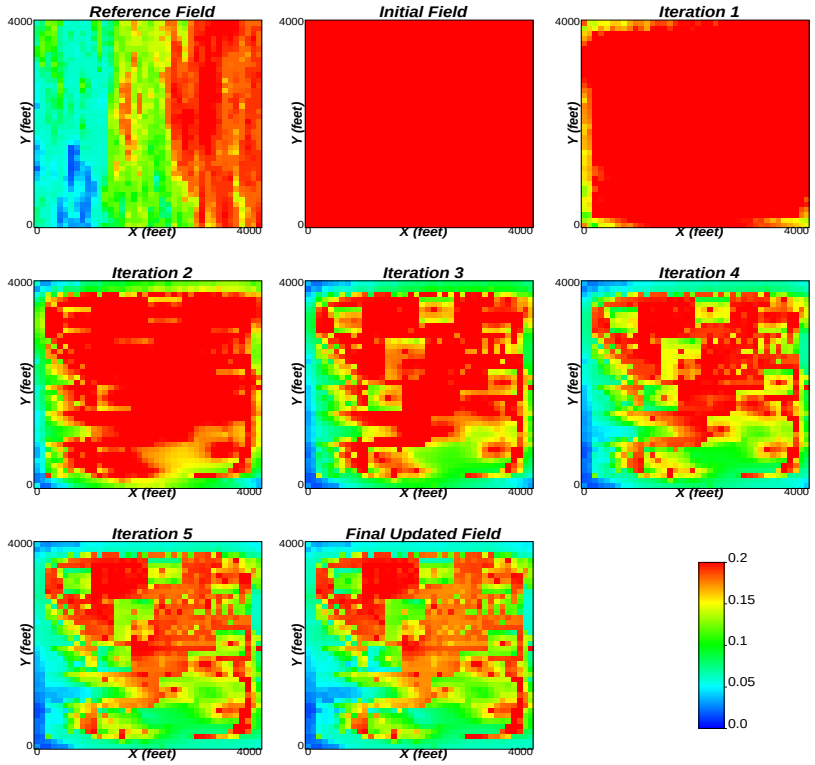

Figure 33: Updated ϕ fields at each iteration of the inversion process: 15 Local Data Case.

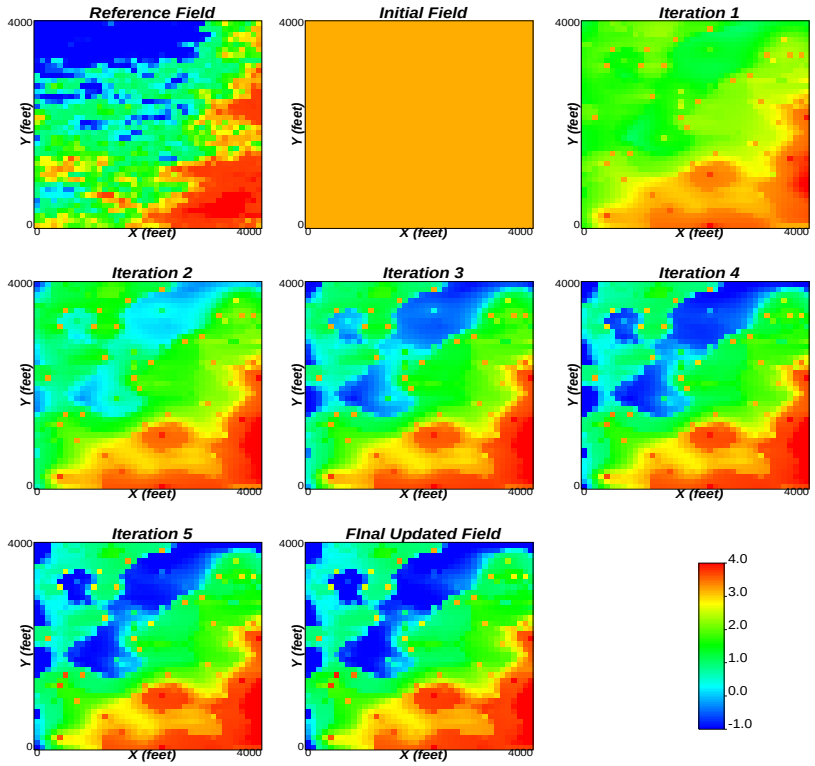

Figure 34: Updated $\ln(k)$ fields at each iteration of the inversion process: 15 Local Data Case.

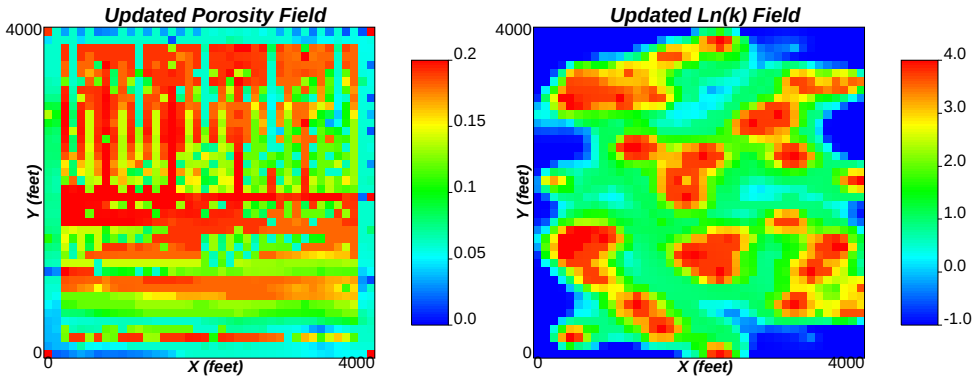

Figure 35: Updated ϕ and $\ln(k)$ fields: No Local Data Case. Poor Convergence.

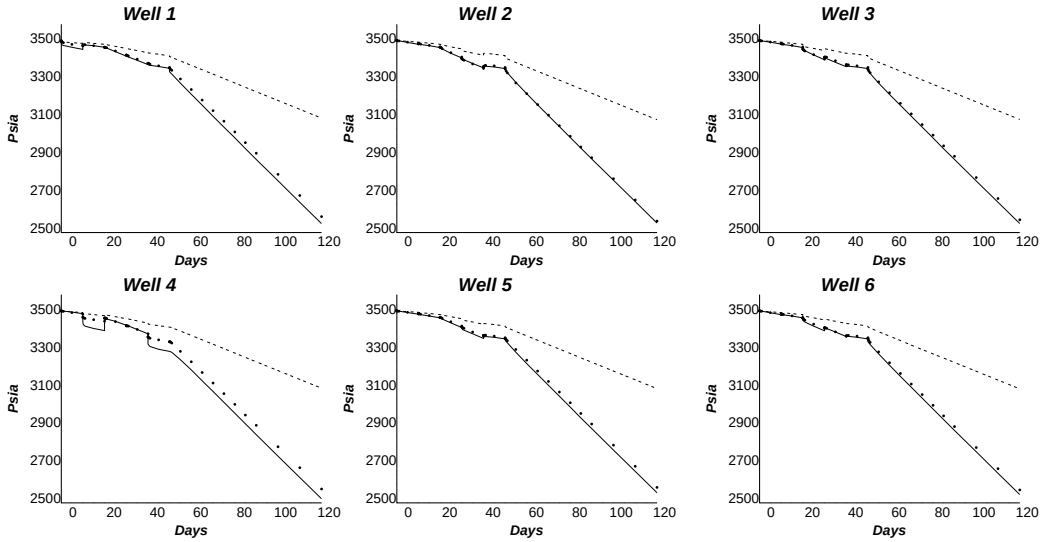

Figure 36: Pressure responses computed from initial (dashed lines) and updated (bullets) ϕ and $\ln(k)$ fields with the true data (solid lines): No Local Data Case.

No Local Data Case

This inversion run was performed without any local data. The inversion was run for 6 outer iterations using 36 master points in each iteration. CPU time for the run was only 115 seconds in a 1.8 GHz Pentium 4 machine. The pressure responses in the updated ϕ and $\ln(k)$ fields do not converge to the reference pressure data. These inverted models are shown in Figure 35. Figure 36 shows the pressure values at the six wells computed from the true (from reference), initial and final updated porosity and permeability fields. The updated fields by the new method accurately reproduce the true pressure data at Wells W2, W3 and W6 only. Well W1 pressure match curve reveals early and late time mismatch indicating improper heterogeneity capture in both the vicinity and the distant grid blocks. Well W4, located at (1750.0, 2650.0), has the greatest mismatch as was evident in most of the previous inversion exercises. The objective function values of the inversion process is shown in Figure 37. It is evident from the figure that realistically no improvement took place after the second outer iteration. It appears that the solution is stuck in some kind of local minimum that is far from the global minimum. Final average pressure mismatch in L^2 norm sense was 17.24 psi, a significantly high value. Updated porosity and permeability fields after each outer iteration of the inversion method are shown in Figures 38 and 39.

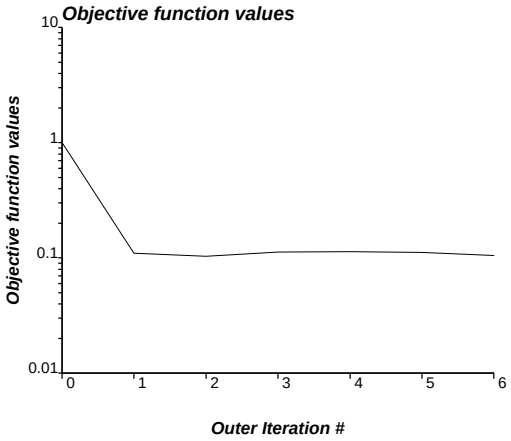

Figure 37: Objective function values of the inversion process: No Local Data Case.

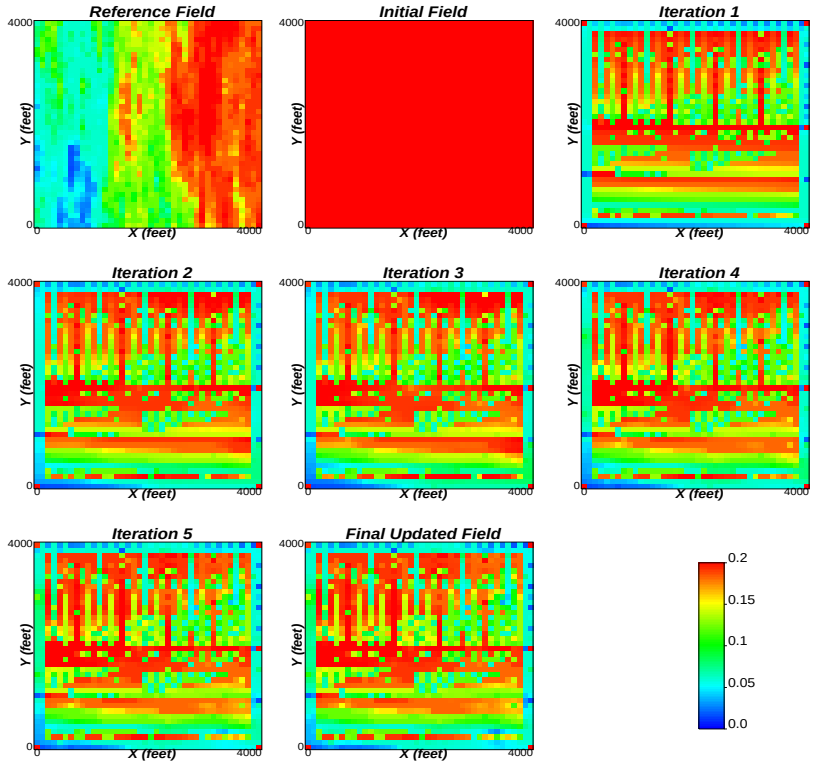

Figure 38: Updated ϕ fields at each iteration of the inversion process: No Local Data Case.

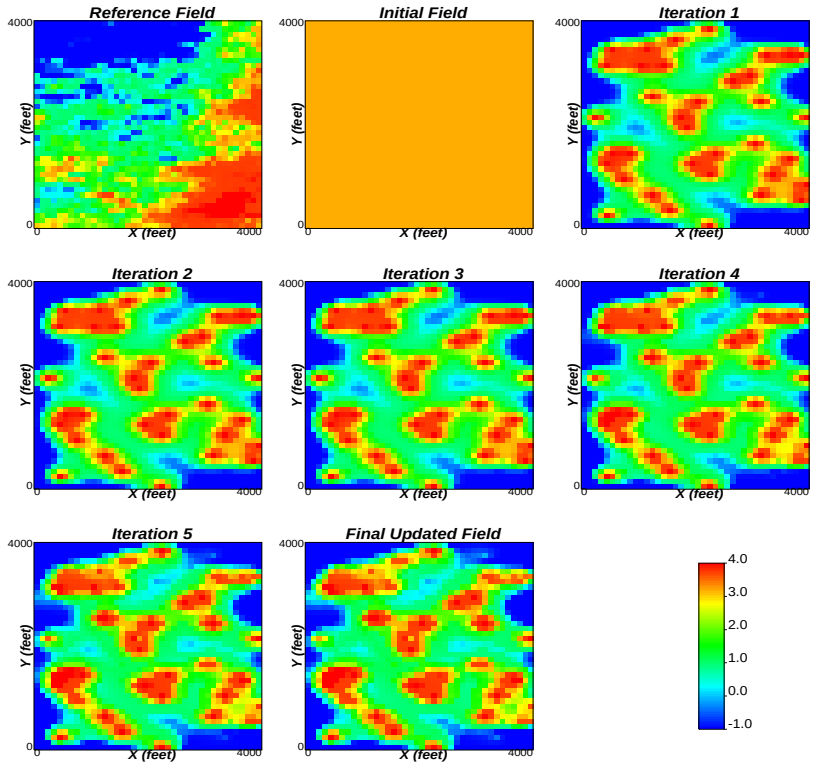

Figure 39: Updated $\ln(k)$ fields at each iteration of the inversion process: No Local Data Case.

Conclusion

From the above sensitivity exercise, it could be concluded that integration of both local data and dynamic production is important for good inverted models. This confirms the hypothesis that different sources of data contain valuable information. One needs to appropriately combine all available information. The extremely poor inversion outcomes in case of no local data reveals that in order to constrain ϕ and $\ln(k)$ values properly, some local data is essential. However, this does not imply that the more the local data being used, the better the inverted models. This is revealed by comparing the cases using 15 and 30 local data cases.

Local data helps regularize the nonlinear inverse problem. The inherent non-uniqueness of inverse problem causes the solution to be stuck in some local minimum unless some regularization scheme is used.

References

[1] Z. A. Reza, X.-H. Wen, and C. V. Deutsch. Simultaneous inversion of porosity and permeability using multiple well production data. In *Report 4*, Edmonton, Canada, March 2002. Center for Computational Geostatistics.